

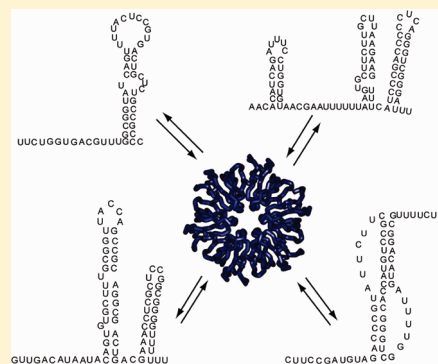
# Despite Similar Binding to the Hfq Protein Regulatory RNAs Widely Differ in Their Competition Performance

Mikołaj Olejniczak\*

Institute of Bioorganic Chemistry, Polish Academy of Sciences, Noskowskiego 12/14, 61-704 Poznań, Poland

**S** Supporting Information

**ABSTRACT:** The binding of nine noncoding regulatory RNAs (sRNAs) to the *E. coli* Hfq protein was compared using a high-throughput double filter retention assay. Despite the fact that these sRNAs have different lengths, sequences and secondary structures their Hfq binding affinities were surprisingly uniform. The analysis of sRNAs binding to Hfq mutants showed that the proximal face of Hfq, known as the binding site for DsrA RNA, is a universal sRNA binding site. Moreover, all sRNAs bound Hfq with similar association rates limited only by the rate of diffusion, while the rates of dissociation, measured in the dilution experiments, were uniformly slow. Despite that, the data showed that there was a hierarchy of sRNAs in regard to their performance in competition for access to Hfq and in their ability to facilitate the dissociation of other sRNAs from Hfq. The sRNAs also differed in their salt dependence of binding to this protein. Overall, the results suggest that despite the uniform binding of different sRNAs to the same site on Hfq their exchange on this protein is dependent on the identities of the competing sRNAs.



Small, *trans*-acting regulatory RNAs (sRNAs) are involved in the response of the bacterial cell to changes in the environmental conditions<sup>1</sup> and affect virulence of several bacterial species.<sup>2</sup> Through the control of translation of specific mRNAs they influence a diverse range of cellular processes, including adaptation to oxidative stress<sup>3</sup> or temperature changes,<sup>4</sup> nutrient metabolism,<sup>5,6</sup> and the protein composition of the outer cell membrane.<sup>7</sup> They repress or, less often, activate translation by pairing with partly complementary regions of their target mRNAs.<sup>8,9</sup> The activity of many of these different sRNAs is dependent on a homohexameric, ring-shaped Hfq protein, which is homologous to eukaryotic Sm proteins.<sup>10,11</sup>

The Hfq protein binds many sRNAs and facilitates their interactions with target mRNAs.<sup>11–13</sup> It is not fully understood how Hfq promotes sRNA–mRNA interactions. One possibility is that Hfq induces such sRNA or mRNA conformations which are favorable for their pairing.<sup>12</sup> Alternatively, the interaction of the partly complementary RNAs could be facilitated by their simultaneous binding to Hfq.<sup>14,15</sup> Moreover, it has been proposed that Hfq is cycled on its RNA ligands<sup>16</sup> and that this cycling may involve an active role for sRNAs.<sup>17</sup> The binding of Hfq to the AU-rich sites in sRNAs or mRNAs was also proposed to protect these RNAs from degradation by RNase E.<sup>18</sup>

Hfq has distinct RNA binding sites on the opposite faces of the ring.<sup>10,14,19,20</sup> The mutations on the proximal side of Hfq are detrimental for binding to DsrA RNA.<sup>14,20</sup> In agreement with that, an AUUUUUG oligoribonucleotide is bound around the central pore on the proximal surface of the *S. aureus* Hfq ring in the X-ray structure.<sup>10</sup> The mutations on the opposite, distal face of the Hfq ring affect the binding of oligoriboadenylates.<sup>14,20,21</sup>

On the basis of the X-ray cocrystal structure of *E. coli* Hfq and A<sub>18</sub>, it was proposed that the distal face is not only the binding site for oligoA but also for RNAs containing a repetitive triplet sequence of adenosine, purine, and any nucleoside residue (ARN)<sub>n</sub>.<sup>19</sup> A repetitive AAN sequence was identified as a very tight Hfq binding site in *rpoS* mRNA and is important for DsrA,<sup>22</sup> RprA, and ArcZ binding to this mRNA both *in vitro* and *in vivo*.<sup>8</sup> Moreover, it has been proposed that *fhlA* mRNA can simultaneously interact with both the proximal and the distal face of Hfq using an (ARN)<sub>n</sub> motif for binding to the distal face.<sup>23</sup> Such a motif was also proposed to be very abundant in *E. coli* genome based on the results of genomic SELEX.<sup>24</sup> Overall, these data indicate that Hfq uses different modes of binding to different RNAs.

Bacterial regulatory RNAs differ in sequence, size, and secondary structure. However, our understanding of Hfq interactions with these RNAs comes mostly from the studies of just one sRNA, DsrA, which has been a subject of intense scrutiny.<sup>14,16,20,25,26</sup> This 85 nt long RNA is composed of three stem loops with an AU<sub>5</sub>G Hfq binding motif in a single-stranded spacer region.<sup>26</sup> Other sRNAs markedly vary in length, typically from about 60 to 120 nt, and they are composed of a varying number of different stem loops, separated by single-stranded regions.<sup>6,7,12,27–29</sup> In one case of sRNA RydC, a pseudoknot structure is formed with two U-rich Hfq binding sites in the loops.<sup>30</sup> Hfq binds to single-stranded regions in sRNAs, which are typically rich in adenosines and uridines. However, the length,

**Received:** December 22, 2010

**Revised:** March 25, 2011

**Published:** April 21, 2011

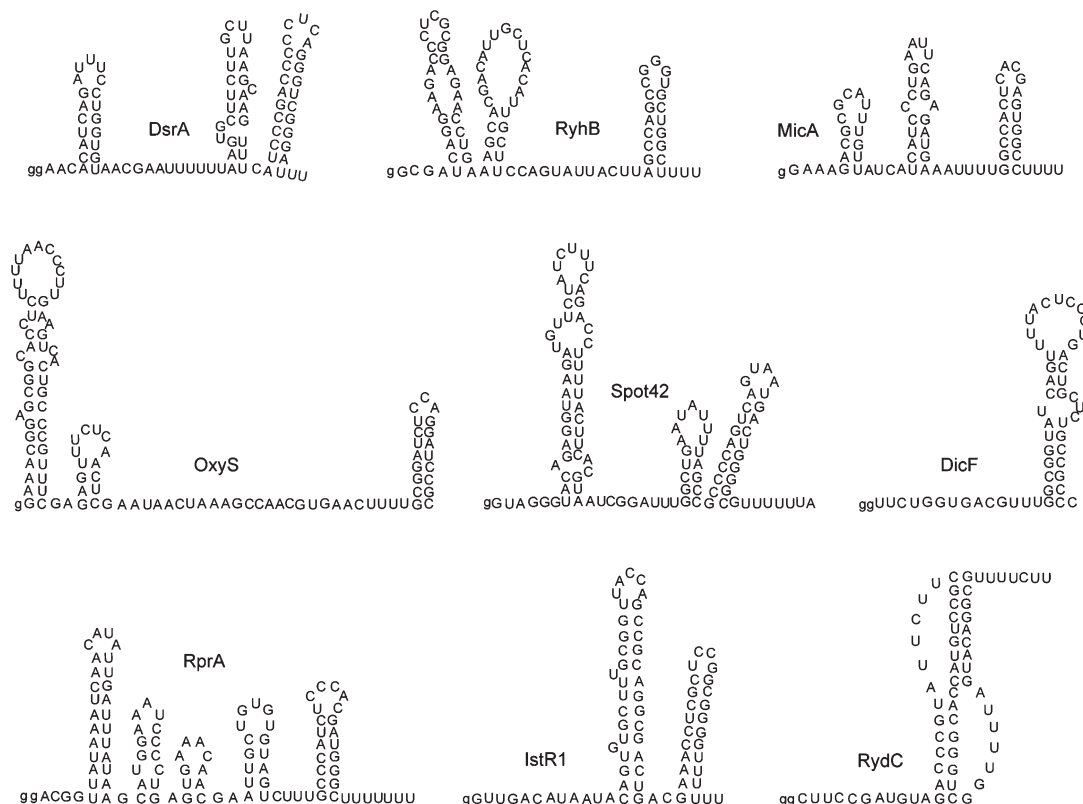


**Figure 1.** *E. coli* regulatory RNAs used in this study. Secondary structures of DsrA,<sup>16</sup> RyhB,<sup>12</sup> MicA,<sup>7</sup> OxyS,<sup>11</sup> Spot42,<sup>6</sup> IstR1,<sup>27</sup> and RydC<sup>30</sup> are presented according to the references, while structures of RprA<sup>28</sup> and DicF are drawn based on the prediction by *mfold*.<sup>39</sup> Guanosine residues added on 5'-ends to ensure the efficiency of *in vitro* transcription are marked with lower case.

sequence, and structural context of these sites widely differ among the sRNAs, and it is not clear whether the Hfq protein uses the same mode of binding to all of them or rather recognizes these different regulatory RNAs specifically.

To better understand how regulatory RNAs are recognized by the Hfq protein nine different sRNAs were selected, which have diverse sequences, lengths, and secondary structures. The thermodynamic and kinetic properties of their binding to the Hfq protein were compared using a high-throughput filter retention assay.

## MATERIALS AND METHODS

**Preparation of RNAs.** sRNAs and the *sodB* mRNA fragment used in this study were prepared by *in vitro* transcription.<sup>31</sup> The sequences of DsrA,<sup>16</sup> IstR1,<sup>27</sup> MicA,<sup>7</sup> OxyS,<sup>11</sup> RprA,<sup>28</sup> RydC,<sup>30</sup> RyhB,<sup>12</sup> and Spot42<sup>6</sup> are the same as in the referenced publications, and the sequence of DicF was obtained from the EcoGene database. Depending on the 5'-end sequence, either one or two guanosine residues were added to the sRNA sequences to enhance transcription yields (Figure 1). Templates for transcription were obtained by the extension of overlapping DNA oligonucleotides (oligo.pl, Warsaw, Poland) using Taq polymerase. RNAs were transcribed with T7 RNA polymerase in a buffer containing 40 mM Tris-HCl pH 8.0, 1 mM spermidine, 0.01% Triton X-100, 20 mM MgCl<sub>2</sub>, 3 mM guanosine, and 2 mM each NTP at 37 °C for 4 h. Reactions were terminated by adding EDTA, pH 8.0, to 25 mM final concentration. Transcripts were purified on 10% denaturing PAGE, excised from the gel, eluted overnight at 4 °C in 0.3 M sodium acetate pH 5.5, 1 mM EDTA,

and ethanol precipitated. After dissolving in water RNAs were stored at −20 °C as 20 μM solutions.

Chemically synthesized oligoribonucleotides A<sub>27</sub>, U<sub>6</sub>, U<sub>18</sub>, and U<sub>51</sub> were kind gifts of Prof. Ryszard Kierzek (Institute of Bioorganic Chemistry, Poznań). The chemically made 27-nt long fragment of gp32 mRNA (mRNA<sub>27</sub>; sequence: 5'-GGC-AAGGAGGUAAAAUG UUCGCACGU-3') and a 49-nt long ribozyme strand of a natural hammerhead obtained using *in vitro* transcription (Hh49; sequence: 5'-UGGGGAUGUGUGUCU-CCACUGAAGA UGGACAAAAGUCCGAAACGUUCCC-3') were kind gifts of Prof. Olke Uhlenbeck (Northwestern University, Evanston, IL).

RNAs were 5'-<sup>32</sup>P-labeled using T4 RNA kinase (Fermentas) and the manufacturer's forward buffer, except for Hh49 which was labeled in the exchange buffer, for 1 h, at 37 °C. Labeling reactions contained 1 μM RNA and 50 μCi 5'-<sup>32</sup>P-ATP (Hartmann Analytic). Labeled RNAs were separated from unlabeled nucleotides using P-30 spin columns (Bio-Rad), followed by ethanol precipitation. Dissolved 5'-<sup>32</sup>P-labeled RNAs were stored at −20 °C as 100 nM solutions.

**Hfq Protein Expression and Purification.** Plasmids for the expression of C-end His<sub>6</sub>-tagged *E. coli* Hfq protein and its mutants were a kind gift of Prof. Andrew Feig (Wayne State University, Detroit, MI). The proteins were expressed and purified essentially as described<sup>14</sup> with the following modifications. After elution from Co<sup>2+</sup> affinity column, fractions containing Hfq were joined, Amicon concentrated, and further purified on HiLoad 200 size exclusion column (GE Lifesciences). The protein was eluted in storage buffer (50 mM Hepes 7.5, 250 mM

NH<sub>4</sub>Cl, 1 mM EDTA, and 10% glycerol), Amicon concentrated, and stored at  $-20^{\circ}\text{C}$ . The purity of the protein was confirmed by SDS PAGE, and the absence of 260 nm absorbing contaminants was confirmed using UV absorbance scan in the 200–300 nm range. The ratio of absorbance at 280 to 260 nm was typically about 1.7. The protein concentration was calculated from absorbance at 280 nm as described.<sup>14</sup>

**Filter Retention Assays.** For double-filter retention assays a 96-well filter block (Minifold, Whatman) was used with the bottom plate modified to increase the filtration rate.<sup>32</sup> Membranes used were top nitrocellulose (Protran, Whatman) and bottom charged nylon (Hybond N+, GE LifeSciences). All reactions were performed and filtered at room temperature ( $25^{\circ}\text{C}$ ). Reaction aliquots were filtered using a multichannel pipet and immediately washed with 100  $\mu\text{L}$  binding buffer. A 25  $\mu\text{L}$  aliquot filtered through the membrane in less than 2 s. After filtration the membranes were hot air-dried, and the intensity of spots quantified using a phosphorimager (Fuji). Data were analyzed using Excel and Kaleidagraph programs.

**Equilibrium Binding Filter Assay.** Binding reactions were performed in Hfq binding buffer (HB buffer; 50 mM Hepes 7.5, 50 mM NaCl, 50 mM KCl, 2.5 mM MgCl<sub>2</sub>, and 0.1 mM EDTA), or the same buffer containing higher monovalent ions concentration where indicated. Immediately before the experiment 5'-<sup>32</sup>P-labeled RNA at 0.1 nM concentration was denatured for 2 min at  $90^{\circ}\text{C}$  in HB buffer without magnesium and then slowly cooled to room temperature. MgCl<sub>2</sub> was added to the final 2.5 mM concentration at the beginning of the renaturation phase. The Hfq solution was prepared by diluting an appropriate amount of Hfq stock into HB buffer. Further dilutions were obtained by sequential 2-fold dilutions to achieve the required range of Hfq hexamer concentrations.

To initiate the binding reaction, 35  $\mu\text{L}$  aliquots of RNA solution were mixed with the same volume of Hfq solution in a microplate. Final 5'-<sup>32</sup>P-labeled RNA concentration in the binding reactions was 50 pM. The reactions were incubated for 30 min at room temperature, and then 50  $\mu\text{L}$  of each binding reaction was filtered and washed with 100  $\mu\text{L}$  of HB buffer. After quantification using a phosphorimager, the data were fit to the Michaelis–Menten binding isotherm. Data were corrected for unspecific retention of RNA on nitrocellulose membrane (less than 2%) in the absence of protein as described.<sup>33</sup>

**Competition Assay.** At first, 6.7 nM Hfq protein was incubated with 8.3 nM cold RNA competitor for 20 min at room temperature in HB buffer, in a 60  $\mu\text{L}$  volume. Subsequently, 20  $\mu\text{L}$  of refolded <sup>32</sup>P-labeled RNA (25 pM final concentration) was added and incubated with the mixture for another 10 min. Final concentrations in the competition reaction were 5 nM Hfq and 6.25 nM cold RNA. Immediately afterward, 70  $\mu\text{L}$  aliquots were filtered and washed with 100  $\mu\text{L}$  of HB buffer. Membranes were dried, and the fraction of RNA bound was determined using phosphorimager.

**Association Assay.** Association reactions were initiated in a microplate by mixing 120  $\mu\text{L}$  volume of refolded <sup>32</sup>P-labeled RNA (5 pM final concentration) with equal volume of Hfq protein at 30–100 pM final concentration range, in HB buffer. Subsequently, 20  $\mu\text{L}$  aliquots were withdrawn at indicated times, immediately filtered, and washed with 100  $\mu\text{L}$  of HB buffer. Also, one 20  $\mu\text{L}$  aliquot of RNA solution without the protein was filtered to control for the background of unspecific RNA retention on nitrocellulose filter. Association rates were calculated from single-exponential fits of fraction bound versus time. Second-order

association rate constants were calculated as linear fits of association rates versus protein concentration.

**Dissociation Assay.** Binding reactions contained 5 nM Hfq and 0.5 nM of refolded 5'-<sup>32</sup>P labeled RNA in HB buffer. After 20 min of incubation 3  $\mu\text{L}$  aliquots of each reaction were transferred to new microplate wells and the dissociation reaction was initiated by adding 297  $\mu\text{L}$  of HB buffer to each well using a multichannel pipet. For some experiments unlabeled RNA was included in the dissociation buffer at indicated concentrations. At indicated times 25  $\mu\text{L}$  aliquots were withdrawn, filtered, and immediately washed with 100  $\mu\text{L}$  of HB buffer. Dissociation rates were calculated as negative slopes of linear fits of natural logarithm of fraction bound versus time. Linear fits and segmental linear fits were performed using Kaleidagraph.

**Gel Shift Assay.** The equilibrium binding reactions of <sup>32</sup>P-labeled RNAs to Hfq were prepared as described above. 9  $\mu\text{L}$  aliquots were withdrawn from the binding reactions, mixed with 3  $\mu\text{L}$  of loading buffer (HB buffer with 15% (w/v) sucrose), and immediately loaded onto a running gel using a multichannel pipet. Samples were resolved on 8% (29:1 acrylamide/bis(acrylamide) ratio) polyacrylamide gel in 0.5  $\times$  TBE buffer at room temperature. Gels were dried and analyzed using a phosphorimager.

## RESULTS

A group of nine *E. coli* regulatory RNAs were selected based on their structural diversity (Figure 1). These sRNAs control different biological processes related to the cell's adaptation to stress.<sup>3,4,6,7,12,27,28,30</sup> Selected sRNAs have 52–109 nt of length and differ markedly with their secondary structures. Most of these RNAs contain short, single-stranded, A/U-rich sequence motifs, which are considered as general Hfq binding sites.<sup>13</sup> However, these regions differ in the sequence and content of adenosines and uridines, and they are embedded in different sequence and structure contexts (Figure 1). The binding of DsrA,<sup>26</sup> MicA,<sup>17</sup> OxyS,<sup>29</sup> RprA,<sup>34</sup> RydC,<sup>30</sup> RyhB,<sup>12</sup> and Spot42<sup>13</sup> RNAs to Hfq have already been observed directly using gelshift assays. Moreover, DsrA, MicA, OxyS, RprA, RyhB, Spot42, and DicF have been reported to coimmunoprecipitate with Hfq, which suggests that they could bind this protein *in vivo*.<sup>35</sup> Hence, eight of these nine RNAs, with the only exception of IstR1, were shown to interact with the Hfq protein. Overall, this group of RNAs provides a diversity necessary to investigate how the Hfq protein interacts with different regulatory RNAs.

A high-throughput double filter retention assay was employed to study the RNA binding to Hfq protein. A single nitrocellulose membrane retention assay has been used before to separate Hfq–RNA complexes.<sup>17,21,36</sup> Adding the bottom charged membrane, which retains free RNAs, allows accurate measurement of the fraction of RNA bound.<sup>33</sup> Additional advantages of this method are the adaptability to the 96-well format with phosphorimager-based data quantification, the possibility to scale up filtered volumes to increase the signal, and very short, less than 2 s, time of complex separation. These properties make this method optimal for comparison of multiple RNAs binding to Hfq, provide a possibility to measure very tight RNA–protein affinities, which requires very low concentrations of RNA, and allow measurement of relatively fast, minute-time-scale kinetics of binding.

**Different sRNAs Bind to Hfq with Similar Binding Affinities.** The results of equilibrium binding experiments show that different regulatory RNAs have similar binding affinities to Hfq hexamer (Figure 2, Table 1). The binding of sRNAs to Hfq was

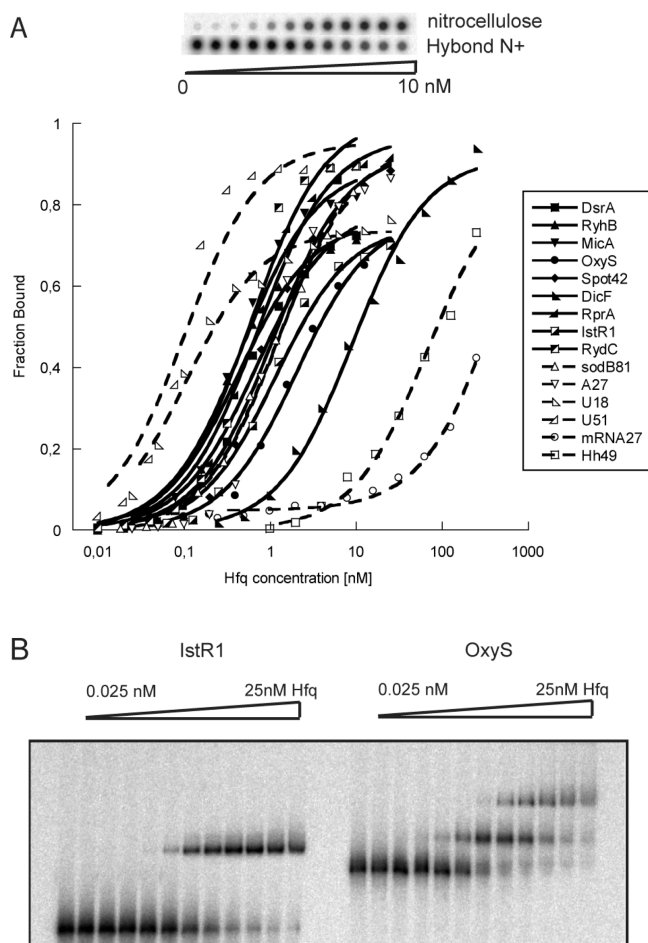


**Figure 2.** Equilibrium RNA binding to *E. coli* Hfq protein. (A) Binding of sRNAs (solid lines, filled or semifilled symbols) and control RNAs (dashed lines, empty symbols) to Hfq using filter retention assay. The lines correspond to the best fits of data. The inset shows raw phosphor-imager data of  $^{32}\text{P}$ -labeled RyhB binding to different concentrations of Hfq. (B) Binding of IstR1 and OxyS sRNAs to Hfq using a gel shift assay.

compared in a low salt Hfq binding buffer (HB buffer), containing total 100 mM concentration of monovalent ions (equimolar NaCl and KCl concentrations). As some sRNAs tend to dimerize in the presence of magnesium,<sup>14,16</sup>  $^{32}\text{P}$ -labeled RNAs were refolded at very low 0.1 nM RNA concentration, which favors single molecule folding. The binding mixture was incubated for 30 min at room temperature before separating Hfq–RNA complexes from free RNAs by filtration. Control experiments showed that increasing the time of incubation in the binding experiment up to 6 h did not make the  $K_d$  values tighter (data not shown). The binding affinities of eight out of nine assayed sRNAs differed less than 5-fold. The binding was very tight with  $K_d$  values in the subnanomolar to low nanomolar concentration range (Table 1). The only exception was DicF RNA, which bound Hfq about 10-fold weaker than other sRNAs. This molecule does not contain a well-defined adenosine and pyrimidine-rich sequence, which may explain the weak binding (Figure 1). The binding affinity of oligoriboadenylate A<sub>27</sub> for Hfq observed here was similar as that of regulatory RNAs, which agrees well with the 2-fold weaker binding in comparison to DsrA RNA that was observed using a gel shift assay.<sup>14</sup> Moreover, the  $K_d$  values of MicA sRNA and A<sub>27</sub> obtained here were very similar as those determined

**Table 1.** Equilibrium Binding of Different RNAs to *E. coli* Hfq and Its Mutants<sup>a</sup>

	wild type Hfq	$K_d$ (nM)		
		Hfq (Y25D)	Hfq (I30D)	Hfq (K56A)
DsrA	0.74 ± 0.4	1.4 ± 0.13	2.1 ± 1.2	180 ± 62
RyhB	0.43 ± 0.18	0.6 ± 0.1	0.52 ± 0.17	52 ± 38
MicA	0.38 ± 0.13	0.72 ± 0.22	0.85 ± 0.51	95 ± 18
OxyS	1.7 ± 1.1	3.5 ± 1.6	5.9 ± 2.3	100 ± 20
Spot42	1.3 ± 0.8	2.1 ± 1	2.1 ± 1.1	160 ± 60
DicF	16 ± 7	22 ± 12	28 ± 13	>250
RprA	1.2 ± 0.5	2 ± 1.1	2 ± 1	130 ± 40
IstR1	0.7 ± 0.34	0.77 ± 0.28	3.6 ± 2.9	150 ± 66
RydC	0.43 ± 0.27	0.93 ± 0.33	0.86 ± 0.56	89 ± 38
sodB81	2.4 ± 1.2	6.5 ± 3.7	37 ± 22	79 ± 51
A <sub>27</sub>	0.87 ± 0.35	>250	>250	6.8 ± 3.1
U <sub>18</sub>	0.13 ± 0.05	0.16 ± 0.06	0.26 ± 0.1	23 ± 0.43
U <sub>51</sub>	0.12 ± 0.06	0.13 ± 0.06	0.11 ± 0.03	0.51 ± 0.28
mRNA27	>250	n.m.	n.m.	n.m.
Hh49	56 ± 35	n.m.	n.m.	n.m.
DsrA-U7	0.54 ± 0.21	n.m.	n.m.	n.m.
RyhB-U8	0.4 ± 0.038	n.m.	n.m.	n.m.
OxyS-U4	0.55 ± 0.071	n.m.	n.m.	n.m.
OxyS-U8	0.26 ± 0.072	n.m.	n.m.	n.m.
MicA-(CA)	0.81 ± 0.28	1.4 ± 0.46	2.4 ± 1.3	>250
MicA-(AAN) <sub>3</sub>	2.1 ± 0.9	2.9 ± 0.9	4.9 ± 1.9	230 ± 40
OxyS-(AAN) <sub>7</sub>	2.5 ± 1.2	20 ± 8	27 ± 7	46 ± 15

<sup>a</sup> Determined for the Hfq hexamer using the filter retention assay in HB buffer (50 mM Hepes 7.5, 50 mM NaCl, 50 mM KCl, 0.1 mM EDTA, 2.5 mM MgCl<sub>2</sub>). n.m. = not measured.

using surface plasmon resonance (SPR)<sup>17</sup> or fluorescence polarization,<sup>19</sup> respectively, in similar binding conditions.

A wider range of Hfq binding affinities was observed for control RNA molecules than for sRNAs (Table 1). While the affinity of an 81 nt long 5'-fragment of sodB mRNA, which contains an Hfq binding site, was similar to that of DsrA sRNA, a 27-nt fragment of gp32 mRNA, which is not a natural target of Hfq, bound Hfq more than 200-fold weaker. Also, the binding of Hfq to a 49-nt long hammerhead ribozyme strand was about 70-fold weaker than to DsrA sRNA. On the opposite end of the affinity spectrum were oligoribourydylates U<sub>51</sub> and U<sub>18</sub>, which bound Hfq at least about 6-fold tighter than DsrA. The tight binding of oligourydylates is in disagreement with the previous observation that Hfq is only weakly retained on polyU cellulose columns.<sup>37</sup> However, it agrees with the fact that polyU effectively outcompetes DsrA RNA from the complex with Hfq.<sup>16</sup> Overall, these experiments show that in the relatively low-salt binding conditions most regulatory RNAs have quite uniform affinities to Hfq, while those RNAs that are not natural ligands of this protein bind with affinities that are either much weaker or much tighter than sRNAs.

To test if the length of the 3' uridine tail, remaining from the Rho-independent transcription termination site, could affect the Hfq binding stabilities of sRNAs the constructs of DsrA, OxyS, and RyhB containing elongated 3' uridine tails were made. DsrA-U7 and RyhB-U8 constructs contained seven and eight uridines, respectively, at the 3' ends. For OxyS two constructs, one with 4 uridines (OxyS-U4) and another with the maximum encoded

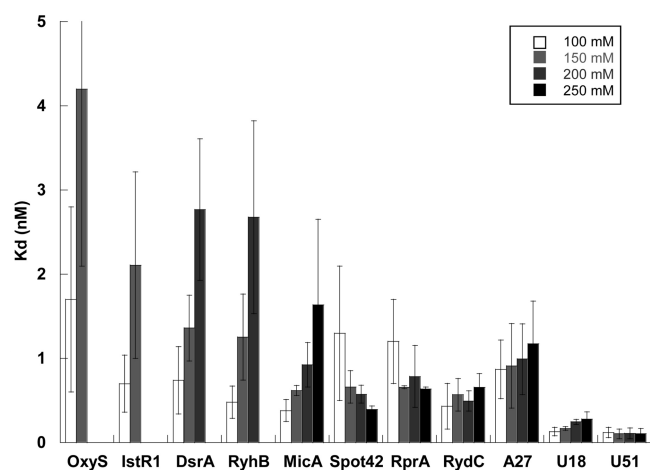


**Figure 3.** Salt dependence of RNA binding to Hfq. Indicated RNAs were incubated with Hfq in buffers containing 100, 150, 200, and 250 mM monovalent ions (equimolar NaCl and KCl).  $K_d$  values were calculated only for the reactions where the maximum fraction bound was higher than 50%. The numbers are averages of at least three independent experiments.

number of eight uridines (OxyS-U8) were made. The equilibrium binding data (Table 1) showed that the effect of the 3' end extension on DsrA-U7 and RyhB-U8 binding was quite small, while OxyS-U4 bound Hfq 3-fold tighter and OxyS-U8 had a further 2-fold effect on binding in comparison to their parental molecules. Overall, the affinities of the extended sRNA constructs were in the same range as those of other sRNAs.

To corroborate the results obtained using the filter retention assay, the binding of sRNAs IstR1 and OxyS to Hfq was analyzed using the gel shift assay (Figure 2B). IstR1 formed one shifted complex with Hfq at the protein concentrations up to 25 nM. The  $K_d$  value of this complex was 1.9 nM (Figure 2B), which is similar to the value obtained using the filter assay (Table 1). The results showed that OxyS formed two complexes with Hfq, in agreement with previous studies.<sup>11</sup> The apparent  $K_d$  value of the aggregate shifted RNA fraction, calculated from data in Figure 2B, was 0.77 nM, which agrees well with the value obtained using the filter assay (Table 1). As the filter assay only monitors the first binding event that is retained on the nitrocellulose membrane, it may be assumed that the  $K_d$  values obtained using the filter assay mostly correspond to the formation of the faster migrating Hfq–sRNA complex. Overall, the  $K_d$  values of IstR1 and OxyS binding to Hfq determined by the gel shift assay were quite similar to one another. This agrees with the conclusion obtained using the filter assay that different sRNAs have similar binding affinities to Hfq.

**Binding of sRNAs to Hfq Is Differently Dependent on Monovalent Ions Concentration.** To further characterize the sRNAs binding to Hfq their dependence on the monovalent ions concentration in the binding buffer was studied using a filter retention assay (Figure 3). However, the data analysis was complicated by the fact that the filter retention of several RNAs was affected by the increased salt concentration. This concerned particularly RyhB, DsrA, OxyS, IstR1, and DicF. This effect was smaller for A<sub>27</sub>, oligouridylylates, RydC, MicA, RprA, and Spot42. For example, with the monovalent ions concentration increase from 100 to 250 mM the maximal fraction retained of A<sub>27</sub> and U<sub>51</sub> (90%) was not affected, while that of RydC changed from 90 to 80%, MicA from 90 to 55%, RyhB from 80 to 30%, and IstR1

from 80 to less than 20% (data not shown). As this could affect the analysis of the binding data, the  $K_d$  values were only determined at these salt concentrations where values of maximum fraction retained for a given sRNA were higher than 50% (Figure 3). It is worth noting that at concentrations of Hfq protein above 25 nM the fraction retained was observed to increase again up to almost 100% at higher salt concentrations for all sRNAs (data not shown). Presumably, this corresponds to the formation of higher order Hfq complexes, which are expected to be better retained on filter at higher salt concentrations than the initial Hfq–RNA complex.

The data show that the binding affinities of regulatory RNAs to Hfq differently depend on the monovalent ions concentration in the binding buffer (Figure 3). The  $K_d$  values of RydC, RprA, Spot42, U<sub>51</sub>, and U<sub>18</sub> were not significantly affected by the increase in monovalent ion concentration from 100 to 250 mM (NaCl and KCl in 1:1 proportion), while the affinity of A<sub>27</sub> decreased less than 2-fold. Indeed, it was previously observed that the affinity of polyA to Hfq decreased only slightly with the increase of NaCl concentration from 0.1 to 1 M, when studied using a nitrocellulose retention assay.<sup>21</sup> At the same time, affinities of IstR1, OxyS, DsrA, RyhB, and MicA were markedly affected by the salt increase in the binding buffer (Figure 3). For example, when monovalent ions concentration was increased from 100 to 200 mM, the affinity of MicA decreased 5-fold and those of RyhB and DsrA decreased 3-fold. Also, the affinity of OxyS and IstR1 decreased almost 3-fold with only the modest increase in monovalent ions concentration from 100 to 150 mM monovalent ions. The observed salt dependence of binding agrees with the results of fluorescence anisotropy studies, which showed that the Hfq binding to AU-rich oligoribonucleotides, derived from DsrA sRNA, was tightest at 100 mM NaCl and weakened dramatically when salt concentration was increased to 300 mM.<sup>38</sup> Similarly, it was shown that the Hfq binding to Q $\beta$  RNA was about 10-fold weaker at 0.3 M NaCl than at 0.1 M NaCl when measured using a nitrocellulose retention assay.<sup>36</sup> Overall, the results presented here show that the Hfq affinity of several sRNAs decreased strongly with the ionic strength of the buffer, while other sRNAs, as well as oligouridylylates and A<sub>27</sub>, were not much affected. This suggests different ionic components of individual sRNAs binding to Hfq and might reflect differences in the way these sRNAs bind to the Hfq protein.

#### Proximal Face of Hfq Is a Universal sRNA Binding Surface.

To compare how different sRNAs are recognized by the Hfq protein, their affinities to Hfq mutants defective with either the proximal or the distal face binding were determined (Table 1). To test for the proximal face binding an Hfq mutant with lysine 56 substituted by alanine was used.<sup>14</sup> The lysine 56 residue (*E. coli* numbering) is located on the proximal face of Hfq, and the K56A mutation is detrimental for the binding of sRNA DsrA to Hfq.<sup>14,20</sup> To test for the Hfq distal face binding two variants of this protein containing either the tyrosine 25 or isoleucine 30 substituted with aspartate were used.<sup>14</sup> Both these residues form part of the R site crevice on the distal face of Hfq, into which purine rings of oligoA are stacked,<sup>19</sup> and are crucial for the binding of A<sub>18</sub> and A<sub>27</sub> to Hfq.<sup>14</sup> As expected, when measured using the filter retention assay (Table 1), the binding affinity of DsrA was not affected by either of the distal face mutations, while the K56A mutant bound this RNA more than 250-fold weaker than wt Hfq did. Conversely, the binding of the A<sub>27</sub> oligoribonucleotide to both proximal face mutants was more than 250-fold weakened, while its affinity to the K56A mutant was only 8-fold decreased. When other sRNAs were tested the results were similar as for DsrA. The binding of RyhB, MicA, IstR1, RydC,

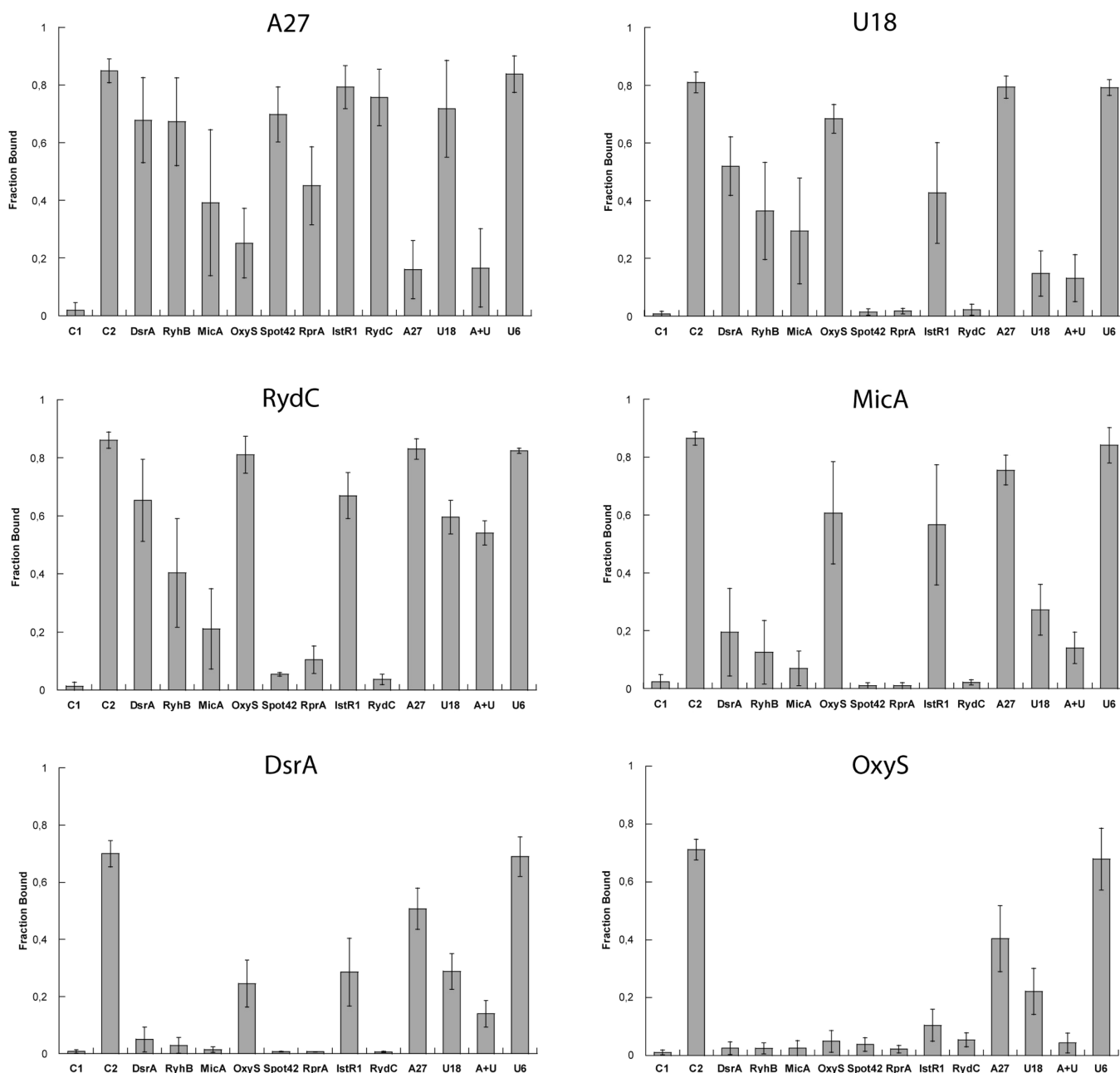


**Figure 4.** Competition for RNA binding sites on the Hfq protein. The graphs show the fraction of  $^{32}\text{P}$ -labeled RNA bound after 10 min of incubation with the complexes of Hfq and unlabeled RNAs. The trace  $^{32}\text{P}$ -labeled RNA whose binding is assayed is indicated on top of each graph. Unlabeled RNAs (at 6.25 nM concentration) which were prebound to Hfq (at 5 nM concentration) are listed below each bar. Control reaction C1 contained only the  $^{32}\text{P}$ -labeled RNA, and C2 contained  $^{32}\text{P}$ -labeled RNA incubated with Hfq in the absence of cold RNA. The fraction bound values are averages of at least three independent experiments.

RprA, Spot42, and OxyS was only slightly or not at all affected by the distal face mutations, while the K56A mutation was always highly detrimental for their binding with effects larger than 100-fold. The 5'-fragment of the *sodB* mRNA (*sodB*81) behaved somewhat differently as its binding to Hfq was affected not only by the proximal face mutation K56A but also by the distal face mutation I30D, but not Y25D, which may suggest a different binding mode of this RNA. The short oligouridylylate  $\text{U}_{18}$  exhibited the same specificity toward the binding site as the regulatory RNAs. Interestingly, the binding of the longer oligouridylylate  $\text{U}_{51}$  was only 5-fold affected by the K56A mutation, and not at all by

the distal face mutations, which suggests that it could bind to both faces of Hfq or use a different set of contacts for binding. Overall, the data indicate that the proximal face of Hfq, shown before as the binding site for DsrA RNA,<sup>14</sup> is the universal binding site for sRNAs.

**sRNAs Occupy the Same Site on Hfq but Differ in Their Competition Performance.** As the use of Hfq mutants only allows detection of the effects of the individual contact points on binding, the binding of labeled sRNAs to different preformed Hfq-sRNA complexes was compared (Figure 4). In these experiments Hfq was first incubated with unlabeled RNA to

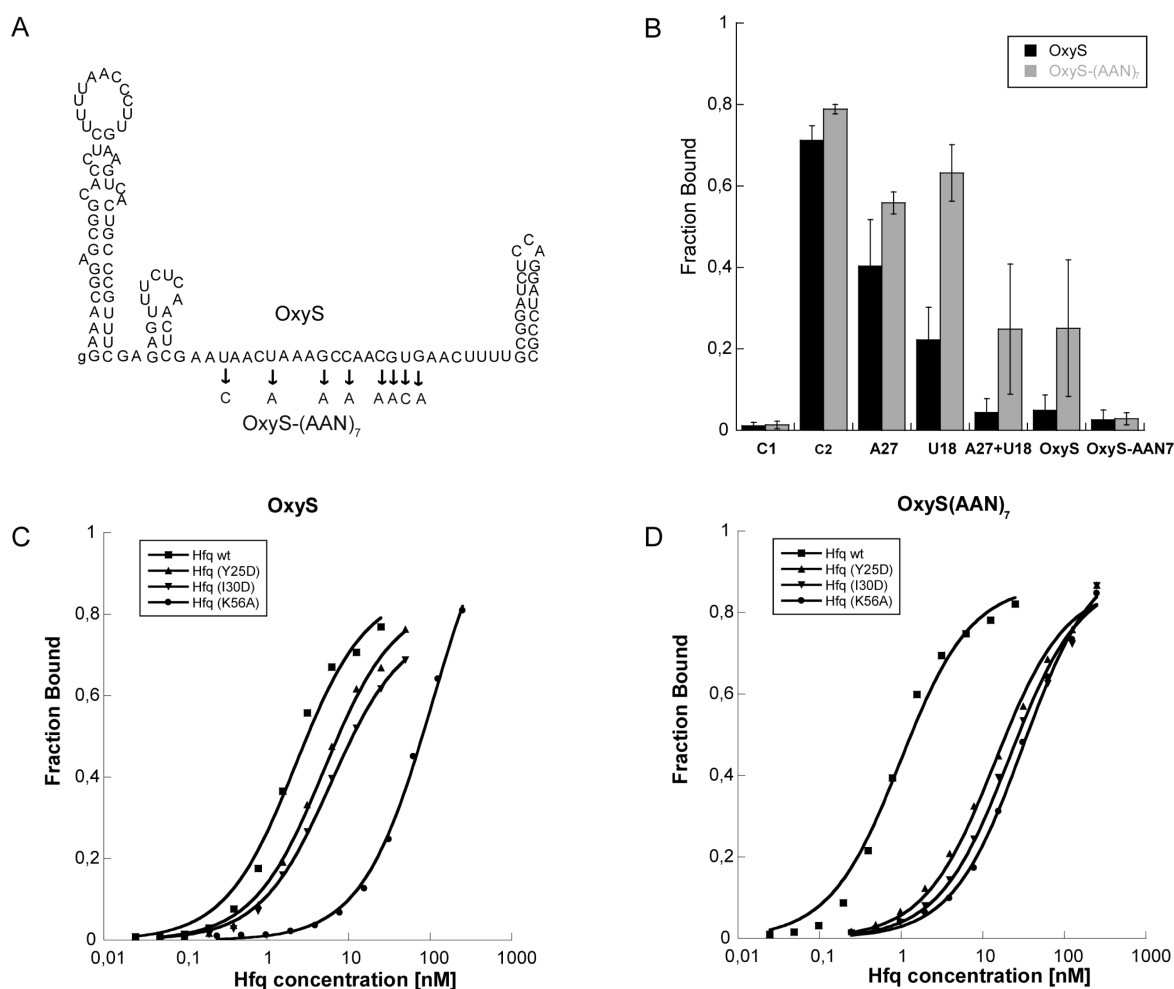


**Figure 5.** Binding of the OxyS mutant with an (AAN)<sub>7</sub> sequence to the Hfq protein. (A) The mutations introduced into the Hfq binding site in OxyS RNA are denoted under the arrows. (B) The fraction bound of <sup>32</sup>P-labeled wt OxyS and OxyS-(AAN)<sub>7</sub> filtered after 10 min of incubation with complexes of Hfq and indicated unlabeled RNAs. Control reaction C1 contained only the <sup>32</sup>P-labeled RNA, and C2 contained <sup>32</sup>P-labeled RNA incubated with Hfq in the absence of cold competitor RNA. (C, D) Equilibrium binding of wt OxyS (C) and OxyS-(AAN)<sub>7</sub> (D) to wt Hfq and its mutants measured by the filter retention assay.

saturate its binding site on this protein. This was followed by a short, 10 min incubation with trace amounts of <sup>32</sup>P-labeled RNA, after which the labeled RNA in complex with Hfq was separated from the free labeled RNA by filtration. Control experiments monitoring the progress of the labeled RNA binding showed that by 10 min the competition reaction already achieved equilibrium (Supporting Information Figure 1). The final concentration of prebound unlabeled RNA in the reaction was 250-fold higher than the concentration of labeled sRNA. At first the control molecules A<sub>27</sub> and U<sub>18</sub> were assayed. A<sub>27</sub> served as a marker of the distal face binding, while U<sub>18</sub> was expected to bind to the opposite side of the Hfq ring. Indeed, the binding of A<sub>27</sub> to preformed unlabeled RNA–Hfq complexes was strongly inhibited only by the unlabeled A<sub>27</sub>. However, it was also moderately inhibited by sRNAs MicA, OxyS, and RprA. Other sRNAs or U<sub>18</sub> did not affect the A<sub>27</sub> binding to Hfq. Conversely, the binding of labeled U<sub>18</sub> to Hfq was not affected by the prebound unlabeled A<sub>27</sub>, which suggests that it binds to the opposite, proximal face of the Hfq ring. However, the labeled U<sub>18</sub> binding was strongly inhibited by sRNAs RydC, Spot42, and RprA, moderately by DsrA, RyhB, MicA, and IstR1 and weakly by OxyS. Importantly, as

there was no effect of A<sub>27</sub> on U<sub>18</sub> binding, and vice versa, it suggests that in the conditions of the assay the labeled RNA pairing with the excess unlabeled RNA does not occur to much extent. This confirms that the observed effects on binding are specific.

The results of the competition assays showed that unlabeled regulatory RNAs differ in their efficiency of preventing <sup>32</sup>P-labeled sRNAs from binding to Hfq (Figure 4). For example, the binding of <sup>32</sup>P-labeled RydC was strongly affected by prebound unlabeled MicA, Spot42, RprA, and RydC itself, moderately by DsrA and RyhB, and weakly or not at all by OxyS and IstR1. A similar relative pattern of effects was observed for <sup>32</sup>P-labeled MicA, DsrA, and OxyS binding. The equimolar mixture of unlabeled A<sub>27</sub> and U<sub>18</sub> had a similar effect on the <sup>32</sup>P-labeled RydC, MicA, and DsrA binding to Hfq as the unlabeled U<sub>18</sub> alone. However, the effect of the A<sub>27</sub>/U<sub>18</sub> mixture was more detrimental for OxyS RNA binding than that of each oligoribonucleotide alone (Figure 4). The competition patterns of other sRNAs were overall similar to those described above (data not shown). In particular, RprA and Spot42 had the same pattern of competition as RydC, while that of RyhB sRNA was virtually identical as DsrA. The extent of binding of labeled IstR1 and DicF

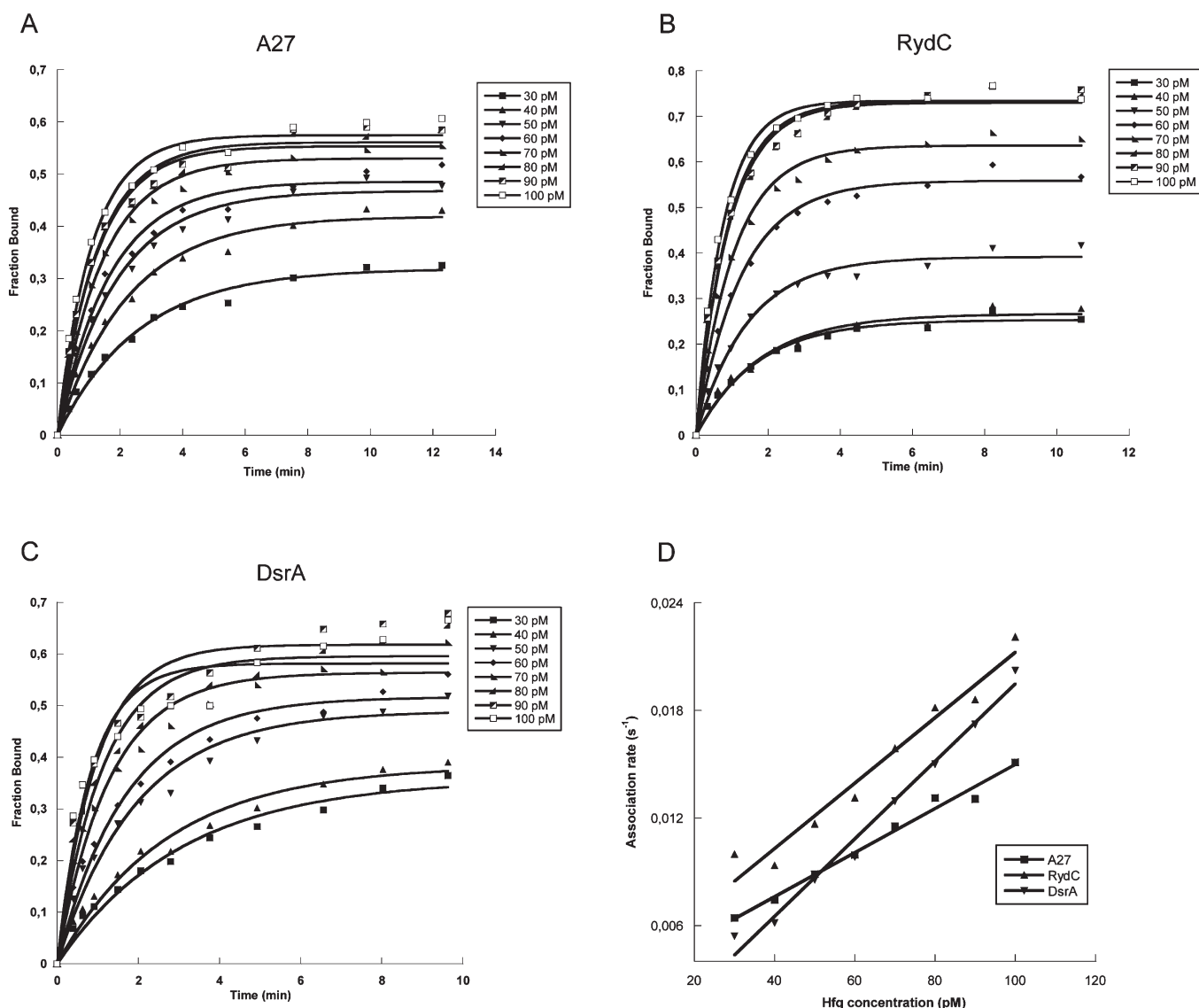


**Figure 6.** Kinetics of RNA association to Hfq. (A–C) Fraction of A<sub>27</sub>, RydC, and DsrA bound to Hfq over time determined by the filter retention assay. The data were fit to a single-exponential equation yielding association rates shown in Table 2 and (D). (D) Second-order plots of association rates from (A), (B), and (C). The slopes of linear fits provide  $k_{on}$  values of  $1.2 \times 10^8 \text{ M}^{-1} \text{ s}^{-1}$  for A<sub>27</sub>,  $1.8 \times 10^8 \text{ M}^{-1} \text{ s}^{-1}$  for RydC, and  $2.2 \times 10^8 \text{ M}^{-1} \text{ s}^{-1}$  for DsrA.

was very low in the presence of all unlabeled RNAs. Overall, the hierarchy of unlabeled sRNAs in preventing the binding of labeled sRNAs to Hfq was IstR1 < OxyS < DsrA < RyhB < MicA < RydC = RprA = Spot42. Besides, the data showed that the effect of unlabeled RNA in complex with Hfq on the binding of <sup>32</sup>P-labeled RNA differed depending on the identity of the labeled RNA. For example, unlabeled DsrA in complex with Hfq decreases the fraction of labeled RydC bound after 10 min incubation to 75%, labeled MicA to 30%, DsrA to about 5%, and OxyS to a level that is undistinguishable from the control without Hfq (Figure 4, Supporting Information Figure 1). Hence, the hierarchy of these four labeled RNAs in regards to their ability to get access to Hfq prebound with unlabeled DsrA is OxyS < DsrA < MicA < RydC.

The competition data show that the binding of all sRNAs was negatively affected by U<sub>18</sub>, and DsrA, but not by A<sub>27</sub>, which suggests that they all bound to the proximal face of Hfq. Besides, when the sRNA constructs with extended 3'-uridine tracts were tested they showed better competition performance than their

parental molecules (Supporting Information Figure 2), which suggests that the 3' terminal uridine tracts participate in sRNA interactions with Hfq. Overall, the differences in the competition performance of sRNAs could suggest that their binding sites differently overlap leading to different accessibility of unlabeled sRNA–Hfq complexes by labeled sRNAs. Alternatively, it could suggest that these differences reflect different extents of exchange of unlabeled sRNAs in complex with Hfq for the labeled ones, which could occur even in the conditions of 250-fold excess of unlabeled RNAs over the labeled ones, and a short time of incubation.

**Mutations in the Sequence of Hfq Binding Site of OxyS sRNA Direct It to the Distal Face of Hfq.** To test if changes in the sequence of Hfq binding sites could direct sRNA molecules to the distal face of Hfq, three sets of mutations were introduced into MicA and OxyS RNAs. At first, it was tested if the presence of uridine residues in the Hfq binding site of MicA is necessary for its binding to Hfq. For that purpose, the AU-rich Hfq binding sequence of MicA (5'-AAAUUUU-3') was changed into an AC-rich one

**Table 2. Association and Dissociation Kinetics of RNA Binding to Hfq<sup>a</sup>**

	$k_{\text{on}}$ ( $\text{M}^{-1} \text{s}^{-1} \times 10^{-8}$ )	$k_{\text{off}}$ ( $\text{s}^{-1} \times 10^4$ ) <sup>b</sup> no chase	$k_{\text{off}}^1$ ( $\text{s}^{-1} \times 10^4$ ) <sup>b</sup> 5 nM chase	$k_{\text{off}}^2$ ( $\text{s}^{-1} \times 10^4$ ) <sup>b</sup> 5 nM chase
DsrA	2.0 ± 0.19	3.2 ± 1.0	64 ± 15	8.8 ± 5.4
RyhB	2.4 ± 0.63	2.7 ± 1.2	52 ± 19	7.9 ± 4.3
MicA	2.3 ± 0.25	1.7 ± 1.1	13 ± 2.3	s.l.
OxyS	0.96 ± 0.24	2.0 ± 0.9	31 ± 8.3	8.2 ± 4.0
IstR1	1.9 ± 0.54	2.4 ± 1.4	6.0 ± 1.7	s.l.
RydC	1.7 ± 0.17	2.1 ± 0.80	11 ± 4.5	s.l.
A <sub>27</sub>	0.88 ± 0.30	3.3 ± 1.8	5.5 ± 2.9	s.l.

<sup>a</sup> Determined using the filter retention assay in HB buffer. <sup>b</sup> Dissociation initiated by 100-fold dilution with or without 5 nM concentration of each respective RNA. s.l. = best fit as a single linear segment.

(5'-ACACAAC-3'), termed MicA-(CA). The length of the single stranded region was the same as in the natural molecule, and the overall secondary structure of the molecule was not changed as judged by *mfold*.<sup>39</sup> This modification resulted in only 3-fold decrease in the binding affinity to wt Hfq and did not affect the MicA-(CA) Hfq binding face specificity (Table 1). Hence, the presence of uridines in the Hfq binding site is not crucial for this sRNA binding to the proximal face of Hfq. Next, a different set of mutations was introduced into the Hfq binding region of MicA, resulting in a change of the natural A<sub>3</sub>U<sub>4</sub> sequence into the 10-nt long 5'-AAAAAAAAAC-3', which could be described as (AAN)<sub>3</sub>. On the basis of the X-ray studies of the complex of Hfq with A<sub>18</sub>, it is expected that RNAs containing a sequence (AAN)<sub>n</sub> would bind to the distal face of Hfq.<sup>19</sup> However, the MicA-(AAN)<sub>3</sub> molecule had only a 4-fold weaker affinity to wt Hfq, and its specificity toward the binding site on Hfq was not changed (Table 1). This could be the result of too short a stretch of AAN repeats, which could only be introduced into the Hfq binding site in MicA without markedly changing the overall structure of the molecule. To test that, a set of eight point mutations was introduced into the long, single-stranded Hfq binding region of OxyS sRNA, resulting in a longer (AAN)<sub>7</sub> sequence (Figure 5A). The secondary structure of the molecule, termed OxyS-(AAN)<sub>7</sub>, was not changed as judged by *mfold* and Pb<sup>2+</sup> structure probing (data not shown). Interestingly, even though the binding affinity to wt Hfq was not much different from that of the natural OxyS RNA molecule, the binding site specificity changed (Figure 5B,C). The mutations Y25D and I30D had a 5-fold stronger detrimental effect on binding than in case of wt OxyS, while the detrimental effect of K56A was 2-fold weaker than for wt OxyS (Table 1). Overall, the OxyS-(AAN)<sub>7</sub> binding to the Hfq(K56A) mutant was only 2-fold weaker than to Hfq(Y25D), while the binding of the natural OxyS molecule to the K56A mutant was 20-fold weaker than to the Y25D mutant. This suggests that an (AAN)<sub>n</sub> sequence may indeed direct RNA binding to the distal face of Hfq, even when it is placed in the context of a structured sRNA molecule. However, its effect may depend on the length and/or the structural context of the repetitive sequence.

**Kinetics of Hfq Binding to Different sRNAs Is Characterized by Diffusion-Limited Association Rates and Very Slow Dissociation Rates.** As the similar binding affinity of different sRNAs could potentially mask the differences in the kinetics of different sRNAs binding to Hfq, the rates of association of six of the RNA molecules to the Hfq protein were compared (Figure 6 and Table 2). As the rates were very fast, it was necessary to

measure them at very low range of Hfq hexamer concentrations, below 100 pM. In this range, the time scale of association was on the scale of several minutes, which is amenable for the manual pipetting based filter assay. The very short, less than 2 s, time of filtration allowed to accurately measure the fraction bound at a given time point. The results showed that the secondary rates of Hfq association to the six sRNAs were very similar to the average  $k_{\text{on}}$  value of  $(1.9 \pm 0.53) \times 10^8 \text{ M}^{-1} \text{ s}^{-1}$  (Table 2). The association rate of A<sub>27</sub> was only 2-fold slower than those of sRNAs. When association of DsrA to 60 pM Hfq was monitored using electrophoresis, only one, fast migrating, Hfq–DsrA complex was observed at this Hfq concentration (Supporting Information Figure 1), which indicates that this rate corresponds to the initial Hfq–RNA complex formation. However, as DsrA was fully bound already at the first time point taken at 30 s, it was not possible to obtain the  $k_{\text{on}}$  value by the gel shift assay. The fact that the rate of association appears faster when measured by the gel shift assay than by the filter assay may reflect the delay between the sample loading and the complete separation of free RNAs from the complex in the gel shift assay conditions. In any way, the very fast rates observed by both assays show that the association of sRNAs to Hfq is limited only by the rate of diffusion.

To further understand the kinetic properties of different RNAs binding to Hfq, the dissociation rates of the six sRNAs and A<sub>27</sub> were measured. The dissociation progress was monitored by diluting the binding reaction by 100-fold and then withdrawing and filtering aliquots at indicated times (Figure 7A and Table 2). The observed similar dissociation rates of sRNAs were very slow with average  $k_{\text{off}}$  value of  $(2.4 \pm 0.54) \times 10^{-4} \text{ s}^{-1}$ . When the  $K_{\text{d}}$  values were calculated from the rates of association and the rates of dissociation ( $K_{\text{d}} = k_{\text{off}}/k_{\text{on}}$ ), the obtained  $K_{\text{d}}$  values were more than 100-fold tighter than the values determined by the direct measurement. For example, the  $K_{\text{d}}$  of RyhB binding measured in the equilibrium experiment was 0.43 nM while the  $k_{\text{off}}/k_{\text{on}}$  ratio was 1.1 pM, resulting in the  $3.8 \times 10^2$ -fold difference. The disagreements between  $K_{\text{d}}$  values measured directly and those calculated from the rates of dissociation and association were observed before for several ribonucleoprotein complexes<sup>40–42</sup> studied by filter retention assays, and it was proposed that this is a signature of the formation of kinetic intermediates in the macromolecular assembly process.<sup>42</sup> Hence, it is possible that the observed disagreement between measured and calculated  $K_{\text{d}}$  values for Hfq–sRNA complex formation indicates that after the initial, filter stable interaction between Hfq and RNA the complex undergoes a further transition, at a rate which is slower than the initial association rate reported by the filter retention assay. If this is the correct explanation, it would mean that the association and dissociation rates monitored by the filter retention assay correspond to different transitions in the process of Hfq–sRNA complex formation.

**sRNAs Differ in Their Ability To Displace Other sRNAs from Hfq.** To further analyze the dissociation kinetics of different sRNA–Hfq complexes, the effect of the presence of unlabeled RNA in the dilution buffer on the progress of <sup>32</sup>P-labeled sRNA dissociation from Hfq was tested. Unlabeled RNA, in high excess over the labeled RNA whose dissociation from a complex is monitored, is often used in the dissociation protocols as a chase, i.e., to prevent the reassociation of dissociated labeled RNA to a protein or a ribonucleoprotein complex.<sup>43</sup> Two very recent papers reported that the off rates of the sRNA MicA, its target *ompA* mRNA,<sup>17</sup> and *fhlA* mRNA<sup>23</sup> from Hfq increased with the concentration of unlabeled chase RNA when studied using nitrocellulose retention assay or SPR experiments. It was proposed that the

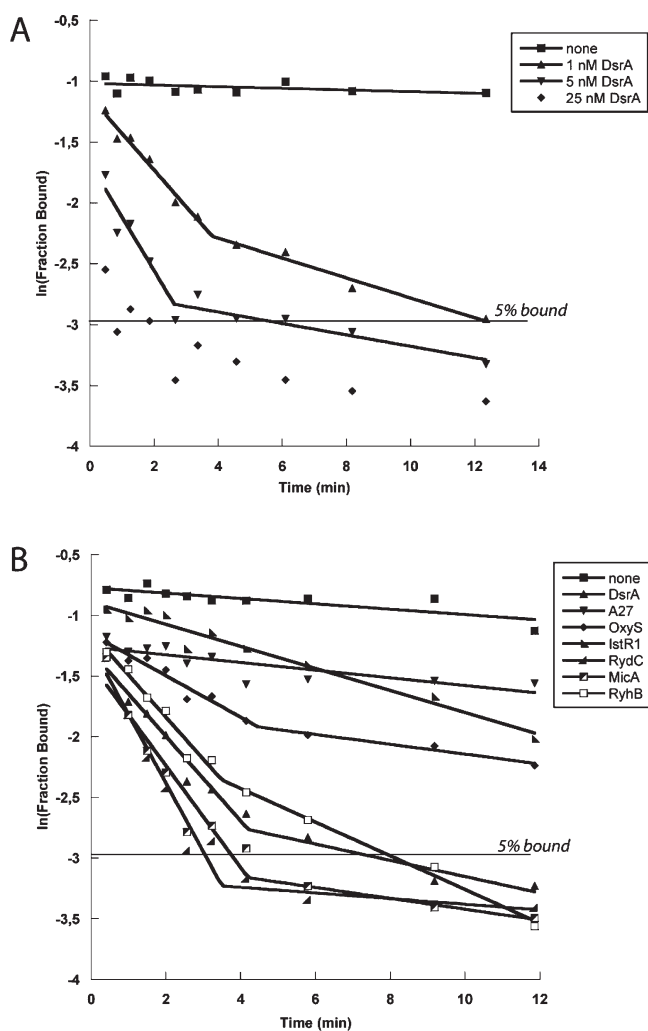


**Figure 7.** Kinetics of DsrA RNA dissociation from Hfq measured by the filter retention assay. (A) The decrease of the fraction of  $^{32}\text{P}$ -labeled DsrA bound to Hfq over time after 100-fold dilution of the Hfq–DsrA complex with solutions containing different concentrations of unlabeled DsrA. (B) Decrease of the fraction of  $^{32}\text{P}$ -labeled DsrA bound to Hfq over time after 100-fold dilution of the Hfq–DsrA complex with solutions containing 1 nM concentration of different unlabeled RNA competitors.

cold chase RNA not only prevents the reassociation of RNA to Hfq but also facilitates the dissociation of labeled RNA from this protein.<sup>17</sup> Here, the dissociation of six sRNAs and A<sub>27</sub> from Hfq was monitored using a high-throughput double filter retention assay after 100-fold dilution with solutions containing respective unlabeled RNAs (Figure 7A). At 5 nM concentration of unlabeled RNAs the rates of dissociation of the respective labeled RNAs were 2–20-fold faster than when dissociation was monitored after dilution with binding buffer only (Table 2). The progress of dissociation of DsrA and RyhB was best fit assuming two linear segments in the plots of  $\ln(\text{fraction bound})$  vs time. At 5 nM unlabeled DsrA, the rate of the first linear segment ( $k_{\text{off}}^1$ ) of DsrA dissociation was 10-fold faster than that of the second segment ( $k_{\text{off}}^2$ ). However, the fraction of labeled DsrA bound was reduced to just 5% at the junction point of the two linear segments, making  $k_{\text{off}}^1$  solely responsible for the dissociation (Table 2). On the other hand, at 1 nM unlabeled DsrA, the junction point corresponded to 10% fraction bound, which made for a somewhat bigger role of

$k_{\text{off}}^2$  in the overall DsrA dissociation. The biphasic progress was observed also for OxyS dissociation at 5 nM chase RNA. However, the junction point of the two segments occurred already at about 80% of the initial fraction bound. At 5 nM concentration of the respective cold RNAs, the dissociation progress of A<sub>27</sub>, IstR1, RydC, and MicA was best fit as single linear.

To corroborate the results of the filter assay, the dissociation progress of DsrA and OxyS RNAs was monitored using a gel shift assay (Supporting Information Figure 2). In this experiment the reassociation was prevented only by the presence of 5 nM unlabeled RNA, without dilution. The binding reaction of 5 nM Hfq with 0.5 nM  $^{32}\text{P}$  labeled DsrA showed only one shifted complex on gel (Supporting Information Figure 2A,B). After the addition of equal volume of unlabeled DsrA to the binding mix the first time point taken at 30 s showed much lower fraction bound than in the binding mix. When the progress of dissociation was presented as  $\ln(\text{fraction bound})$  vs time, including the “zero” time point taken immediately before the start of dissociation, the dissociation progress could be approximated as two linear segments corresponding to  $k_{\text{off}}^1$  of  $140 \times 10^4 \text{ s}^{-1}$  and  $k_{\text{off}}^2$  of  $12 \times 10^4 \text{ s}^{-1}$  (Supporting Information Figure 2C), which are similar to the values obtained using the filter assay (Table 2). The binding reaction of 5 nM Hfq and 0.5 nM  $^{32}\text{P}$  labeled OxyS showed two shifted complexes with 80% of labeled OxyS in the higher order complex (Supporting Information Figure 2A,B). When the binding reaction was mixed with an equal volume of unlabeled OxyS at final 5 nM concentration, the higher order complex was mostly dissociated before the first time point of 30 s, and the majority of label was in the lower molecular weight complex. Hence, the dissociation of the OxyS–Hfq complex begins with the dissociation of the higher order complex to the lower order one, which is followed by the release of free RNA from the lower molecular weight complex. When the aggregate shifted fraction was plotted as  $\ln(\text{fraction bound})$  vs time, it fit linearly with the  $k_{\text{off}}$  value of  $10 \times 10^4 \text{ s}^{-1}$  (Supporting Information Figure 2C), which is similar to the  $k_{\text{off}}^2$  value determined for OxyS using filter assay (Table 2). These confirm that the presence of unlabeled RNA increases the rate of sRNA dissociation from Hfq. However, they also underline the fact that as certain sRNAs form higher order complexes with this protein, their dissociation may involve several transitions.

If regulatory RNAs can ease their own dissociation from Hfq, it is interesting if they could also ease other sRNAs dissociation from this protein. Such a mechanism could be important during the regulation of bacterial response to environmental stimuli happening simultaneously or following shortly one after another. To test that, the progress of dissociation of  $^{32}\text{P}$ -labeled DsrA from Hfq was monitored after 100-fold dilution with solutions containing one of six different sRNAs or A<sub>27</sub> at 1 nM concentration (Figure 7B and Table 3). As expected, the presence of unlabeled A<sub>27</sub> did not affect the dissociation of DsrA. However, all sRNA competitors affected its dissociation with rates dependent on the identity of a given sRNA. The progress of DsrA dissociation in the presence of most competitors had two components, which suggests that the complexes were not entirely homogeneous (Figure 7B). However, as the second component corresponded to a very small fraction (about 5%) of the total, only the dissociation rate values of the first, dominant component ( $k_{\text{off}}^1$ ) are presented in Table 3. The hierarchy of sRNAs in relation to their efficiency at inducing the dissociation of the Hfq–RNA complex was the same for Hfq complexes with  $^{32}\text{P}$ -labeled DsrA, RyhB, or OxyS, and it was IstR1 < OxyS < DsrA = RyhB < MicA = RydC (Table 3). These results

**Table 3. Dissociation of DsrA, RyhB, and OxyS Induced by Competitor RNAs<sup>a</sup>**

competitor RNA <sup>b</sup>	dissociation of 5'- <sup>32</sup> P-labeled RNA from Hfq (s <sup>-1</sup> × 10 <sup>4</sup> ) <sup>c</sup>		
	DsrA	RyhB	OxyS
none	2.9 ± 0.97 <sup>d</sup>	2.9 ± 1.3 <sup>d</sup>	2.0 ± 0.97 <sup>d</sup>
DsrA	64 ± 16	48 ± 8.4	42 ± 21
RyhB	59 ± 1.5	52 ± 19 <sup>d</sup>	40 ± 5.2
MicA	65 ± 7.3	58 ± 4.9	46 ± 6
OxyS	20 ± 7	35 ± 2.8	31 ± 8.3 <sup>d</sup>
IstR1	12 ± 4.5	12 ± 3.1	6.5 ± 2.7
RydC	78 ± 25	63 ± 13	48 ± 10
A <sub>27</sub>	6.3 ± 1.4	2.0 ± 1.2	3.0 ± 1.7

<sup>a</sup> Determined using the filter retention assay in HB buffer. <sup>b</sup> Competitors were used at 1 nM concentration for DsrA and 5 nM for RyhB and OxyS RNAs. <sup>c</sup> Dissociation measurement was initiated by 100-fold dilution of the sample with indicated cold RNA solution,  $k_{\text{off}}$  values in the presence of DsrA, RyhB, MicA, RydC, and OxyS correspond to the initial dissociation rates ( $k_{\text{off}}^1$ ), and others were fit single linear. <sup>d</sup> Data from Table 2.

suggest that despite similar affinities to Hfq these sRNAs have different properties in competing with other sRNAs for access to this protein.

## DISCUSSION

The results presented here show that despite very different sequences and secondary structures (Figure 1) regulatory RNAs bind to Hfq with similar affinities, when tested in the same binding conditions (Figure 2 and Table 1). The  $K_d$  values determined here are in the subnanomolar to low nanomolar range (Table 1), which is tighter than sRNA affinities to Hfq observed in most studies,<sup>6,12,14</sup> but agrees well with the  $K_d$  values determined by SPR for MicA<sup>17</sup> and by fluorescence anisotropy for oligoA,<sup>19</sup> in similar binding conditions. On the other hand, a wide range of Hfq binding affinities have been reported for several sRNAs.<sup>12–14,17,20,26</sup> For example, the gel shift determined affinity of RyhB for Hfq was 250 nM,<sup>12</sup> the  $K_d$  value of DsrA RNA was 21 nM,<sup>14</sup> and the  $K_d$  of MicA binding to Hfq, calculated from kinetic rates of association and dissociation obtained by SPR, was just 0.5 nM.<sup>17</sup> Part of the explanation for this variability could be the different dependence of RNA binding to Hfq on salt concentration. Indeed, it was observed here that the affinity of OxyS, IstR1, DsrA, RyhB, and MicA decreased strongly with increasing monovalent ions concentration (Figure 3). Salt dependence of Hfq binding was also observed for AU-rich oligoribonucleotides<sup>38</sup> and Q $\beta$  phage RNA.<sup>36</sup> Also of particular importance for the accuracy of Hfq binding assays are the details of the Hfq purification protocol, especially the treatment with DNase and RNaseA to remove contaminating nucleic acids.<sup>14,44</sup> Besides, the measured affinities could be affected by different RNA concentrations used in the binding assays because the dissociation rates of Hfq–RNA complexes depend on RNA concentration (Figure 7A and Table 2).<sup>17,23</sup> Another factor could be the presence of carrier tRNA in the binding mixtures, as the  $K_d$  of RydC binding to Hfq increased from 20 to 80 nM with carrier tRNA concentration,<sup>30</sup> and Hfq was observed to bind tRNAs quite tightly.<sup>45</sup> Finally, because many sRNAs contain long single-stranded regions, their structures may be quite dynamic, as it was observed for

DsrA RNA,<sup>46</sup> and hence susceptible to even small differences in experimental conditions, which could affect Hfq binding. Overall, it appears that in spite of the fact that Hfq protein is very thermally stable and remains bound to its RNA ligands even in the conditions of 7 M urea PAGE (ref 26, data not shown), its binding properties are very sensitive to the details of the experimental protocol.

The proximal face of Hfq appears to be a universal sRNA binding site (Table 2 and Figure 4). Previous studies indicated that the proximal face of Hfq is the binding site for DsrA RNA,<sup>14</sup> and its fragments,<sup>20</sup> while the *hflA* mRNA was proposed to bind to both sides of the torus.<sup>23</sup> The binding of RprA sRNA to Hfq was 5-fold weakened by a proximal face mutation F39A and 3-fold by the distal face mutation Y25A.<sup>34</sup> Moreover, the mutations on both sides of Hfq were detrimental for the Hfq facilitated annealing of DsrA-derived oligoribonucleotide with a molecular beacon.<sup>15</sup> On the other hand, short oligoribonucleotides derived from DsrA and *rpoS* mRNA competed for binding to a single site on Hfq.<sup>47</sup> The data obtained here show that all nine studied sRNAs are sensitive to the K56A mutation on the proximal surface of Hfq, while the distal face mutations Y25D and I30D did not affect their binding (Table 1). This conclusion is supported by the results of the competition studies (Figure 4), which showed that the binding of most sRNAs is not sensitive to the saturation of Hfq with A<sub>27</sub>, which binds to the distal surface of the protein. However, all nine sRNAs are sensitive to the saturation of Hfq binding sites with other sRNAs and U<sub>18</sub>, which bind to the opposite site of Hfq than A<sub>27</sub>. The results reported here did not confirm the effect of the mutation in the Hfq position 25 on RprA binding.<sup>34</sup> One explanation could be differences in the sequences of RprA molecules used,<sup>34</sup> which could affect the details of the contacts formed between this sRNA and the Hfq ring. However, the competition assay data showed that the binding of A<sub>27</sub> to Hfq is indeed moderately affected by RprA, MicA, and OxyS sRNAs (Figure 4). This suggests that the distal face contacts may be involved in their interactions with Hfq.

Interestingly, when OxyS was mutated in eight positions to introduce an (AAN)<sub>7</sub> repeated sequence in its Hfq binding site it became sensitive to the distal face mutations, suggesting a switch in the Hfq face binding specificity of this RNA (Figure 5). This confirms the conclusions of the X-ray studies<sup>19</sup> and a recent SPR study<sup>23</sup> that (ARN)<sub>*n*</sub> sequences, which were proposed to have important roles in Hfq interactions with mRNAs,<sup>8,22–24</sup> serve to direct RNAs to the distal face of the protein. However, as the introduction of a shorter (AAN)<sub>3</sub> sequence into the Hfq binding site of MicA did not affect its Hfq face specificity, it suggests that the effect of (AAN)<sub>*n*</sub> sequence on Hfq binding may depend on the length of the repeated sequence or the surrounding RNA structure. Overall, the mutant binding and competition data indicate that the proximal face of Hfq is a universal sRNA binding site and support the role of (ARN)<sub>*n*</sub> motifs in directing RNAs to the distal site.

The data presented here show similar, very fast rates of Hfq association to sRNAs, limited only by the rate of diffusion (Figure 6 and Table 2). The association rates observed here were on the order of 10<sup>8</sup> M<sup>-1</sup> s<sup>-1</sup>, which corresponds to the diffusion rate limited maximum. These rates are much faster than the association rates observed by SPR for *hflA* mRNA,<sup>23</sup> *ompA* mRNA, and MicA sRNA binding to Hfq,<sup>17</sup> which were on the order of 10<sup>6</sup> M<sup>-1</sup> s<sup>-1</sup>. However, a comparable rate of 6.9 × 10<sup>7</sup> M<sup>-1</sup> s<sup>-1</sup> was recently obtained using fluorescence stopped flow experiments for an AU-rich oligoribonucleotide binding to Hfq.<sup>15</sup> One possible explanation for these differences could be that the first binding event that is filter stable is different than the

one monitored by SPR. Indeed, similarly fast rates as observed here were determined before for the formation of other ribonucleoprotein complexes, including the interaction between bI3 maturase and group I intron RNA, which was also studied using a filter retention assay.<sup>40</sup> One reason for the very fast rates of Hfq–RNA association could be the presence of six identical RNA binding sites on the surface of Hfq homohexamer, which increases the chances of effective encounters. Moreover, such very fast, diffusion-limited association rates suggest that sRNAs do not need to undergo a conformational change before forming the first filter stable interaction with Hfq.

As the equilibrium dissociation constants determined directly in filter binding experiments (Table 1) were about 2 orders of magnitude weaker than those calculated from rates of association and dilution-monitored dissociation, this could mark the presence of intermediate steps in the path of sRNA association to Hfq.<sup>40,42</sup> Indeed, the fluorescence study of DsrA-derived oligonucleotides binding to Hfq showed that the association proceeded in two steps, the first of which occurred with a rate similar to that observed here, and the second one was much slower.<sup>15</sup> A two-step association was also recently proposed for *fhlA* mRNA binding involving both faces of Hfq.<sup>23</sup> The presence of multiple steps in the path of sRNA association to Hfq is also in agreement with a recently proposed model of sRNA exchange on Hfq.<sup>17</sup>

Although the different Hfq–sRNA complexes dissociate with uniformly slow rates when monitored after dilution only, the rates significantly increase in the presence of chase RNA. The  $k_{\text{off}}$  values obtained here for unassisted dissociation were on the order of  $10^{-4} \text{ s}^{-1}$  (Table 2), which is very similar to the rates observed for MicA sRNA and *fhlA* mRNA using filter assays and SPR, respectively.<sup>17,23</sup> However, all six assayed sRNAs showed faster dissociation rates at increased RNA concentrations (Figure 7A and Table 2). Indeed, it was previously observed that the addition of *sodB* mRNA to the ternary *sodB* mRNA–RyhB–Hfq complex resulted in the release of the binary *sodB* mRNA–RyhB complex, leading to a hypothesis that Hfq recycling occurs via its interactions with other Hfq ligands.<sup>48</sup> Besides, it was proposed that Hfq is cycled on DsrA RNA, and rapid DsrA dissociation from Hfq was observed in the presence of polyU competitor.<sup>16</sup> In agreement with this, the dissociation of *fhlA* mRNA from Hfq was 50-fold faster in the presence of A<sub>18</sub> and DsrA RNAs than when monitored only by buffer flow in the SPR experiment.<sup>23</sup> Finally, it has been recently proposed that sRNAs play an active role in their cycling on Hfq.<sup>17</sup> According to this hypothesis the incoming RNA binds to the RNA–Hfq complex, and by occupying an increasing number of RNA binding sites on the hexamer, it facilitates the dissociation of the previously bound RNA.<sup>17</sup> Regardless of the detailed mechanism, it appears that the dependence of Hfq–RNA complex dissociation on RNA concentration would allow efficient exchange of sRNAs on Hfq, especially at increased sRNA concentrations during response to stress.

The RNA concentration dependence of the RNA–protein complex dissociation was observed also for another homohexameric RNA binding protein—Rho terminator of transcription.<sup>49,50</sup> Similarly as Hfq, this protein binds its RNA ligands very tightly and shows very slow rates of dissociation in the absence of chase RNA. However, the rates increase depending on the RNA concentration, and it was proposed that the overall dissociation rate of RNAs from Rho includes the components of the true dissociation rate and the pseudo-first-order rate of displacement.<sup>49,50</sup> Hence, it is possible that the dependence of dissociation rates on the RNA

concentration may be a general property of certain homohexameric RNA binding proteins.

Despite the similar strength of binding at equilibrium, as well as uniform kinetics of association and unassisted dissociation, regulatory RNAs perform differently in the competition for binding to Hfq (Figures 4 and 7B, Table 3). The hierarchy of unlabeled sRNAs in their efficiency of preventing labeled sRNA from binding to the preformed complex observed here was IstR1 < OxyS < DsrA < RyhB < MicA < RydC = RprA = Spot42 (Figure 4). Besides, the results showed that the labeled sRNAs dissociated from Hfq with the rates dependent on the identity of the competing sRNAs (Figure 7B, Table 3), and the hierarchy of competitors was virtually the same as that established in the first kind of competition assay (Figure 4). The competition among sRNAs for access to Hfq has already been suggested by several papers. In agreement with the relative competition performance proposed here, it has been reported that OxyS was less effective than DsrA in displacing labeled DsrA from the complex with Hfq.<sup>51</sup> Besides, it was shown that IstR1 was inefficient in displacing MicA sRNA from the complex with Hfq, similarly as observed here.<sup>17</sup> Also, MicF was shown to be a better Hfq competitor than MicA or MicC sRNAs,<sup>17</sup> which suggests that the competition for access to Hfq occurs also among sRNAs regulating the outer membrane proteins expression.

The differences in the competition performance among sRNAs likely reflect their ability to actively displace other sRNAs from Hfq. Although it could theoretically be possible that the differences in competition arose from the different extents of overlapping of the binding sites of competing sRNAs, it does not seem likely. For example, even though the prebound RydC effectively prevents labeled DsrA from binding to Hfq, the opposite is not true as the prebound DsrA does not prevent labeled RydC from binding (Figure 4). Hence, it seems more likely that the reason for differences in competition is that some sRNAs are better than others at actively displacing RNAs from Hfq as suggested by the results of the competitor RNA-induced dissociation assays (Figure 7B). Either of these explanations would require at least a transient formation of a ternary complex with both sRNAs bound to Hfq. However, a presence of such a complex was not detected when the dissociation was monitored in the presence of chase RNA using a gel shift assay (Supporting Information Figure 4), presumably because of its transient nature.

The structure of studied sRNAs may differently contribute to their competition performance. It appears that the least structured sRNAs IstR1, DicF, and OxyS are also the least efficient competitors (Figures 1 and 4, data not shown). This could be related to the previous observation that Hfq binding sites in sRNAs require stem-loop structures on both sides of the single-stranded AU-rich sequence.<sup>26</sup> This is not the case for IstR1 and DicF, and in OxyS the stem loops are quite distant from the AU-rich sequence (Figure 1). Possibly the less structured sRNAs have a smaller area of contact on the Hfq surface, making them less efficient competitors. It appears that the length of the 3' terminal uridine tracts may also play a role in competition, as the sRNAs with extended 3' uridine tracts were better competitors than their parental molecules (Supporting Information Figure 2). Possibly a longer 3' uridine tract would make it easier for an sRNA to load onto Hfq and displace an already bound sRNA. On the other hand, when IstR1, RyhB, DsrA, and MicA, which have a similar 3' tail length of 3–6 uridines, are compared (Figure 1), a range of competition efficiencies is observed (Figures 4 and 7B), which suggests that other properties of their structure are also important.

Interestingly, the salt dependence of the Hfq binding appears to predict sRNA competition performance. For example, the weak competitors IstR1 and OxyS were the most affected by the salt increase in the binding conditions, which would suggest a larger electrostatic component of binding,<sup>52</sup> while the strong competitors MicA and RydC were the least affected by it (Figure 3). Hence, it is possible that the differences in competition performance reflect differences in the kind of interactions formed between Hfq and these sRNAs.

The competition among sRNAs for access to Hfq has also been suggested *in vivo*. Even though Hfq is a very abundant protein in bacterial cells, it was recently shown that its concentration is a limiting factor for regulation by DsrA, RyhB, OxyS, and MicC sRNAs in *E. coli*.<sup>53</sup> Moreover, when unpartnered sRNAs or mRNAs were overexpressed, the activity of all four sRNAs in regulating their target mRNAs was disrupted. This effect was reversed upon overexpression of Hfq, suggesting that the competition among these RNAs for access to Hfq caused this effect.<sup>53</sup> In a separate study, the deep sequencing methodology was used to reveal that the overexpression of ArcZ sRNA in *Salmonella* resulted in the reprofiling of Hfq bound sRNAs. The binding of some sRNAs, including RprA, Spot42, and MicA, was decreased, while that of others, among them DsrA, OxyS, and RydC, was increased, which could suggest competition among these sRNAs for Hfq.<sup>54</sup> Overall, these data indicate that the competition for access to Hfq may have important role in sRNA-dependent translation regulation *in vivo*.

The function of Hfq protein in bacterial cells depends on its binding to different kinds of RNA targets. Besides regulatory RNAs, the ligands of Hfq include polyA tails, mRNAs, tRNAs, and possibly also other molecules, including the ribosome. The data presented here show that Hfq binds different sRNAs with similar, subnanomolar affinities, and uniform kinetics of association and dilution-induced dissociation. As Hfq is one of the most abundant proteins in the cell with the concentration similar to that of the ribosomes,<sup>55</sup> it might appear that such tight affinities would not be biologically relevant. However, because Hfq binds so many abundant targets, it may be assumed that its free concentration is much lower, which would make the tight Hfq binding necessary to retain bound regulatory RNAs for the mRNA targeting. The data presented here show that there is a hierarchy of sRNAs in relation to their efficiency in replacing sRNAs bound to Hfq, which may affect the response of bacterial cell to environmental changes that are mediated by the competing sRNAs. The similar binding of different sRNAs to the same site on Hfq may be a necessary requirement for their efficient recycling, which is further modulated by the individual properties of each sRNA, thus allowing for the flexible bacterial cell adaptation to changing environmental conditions.

## ■ ASSOCIATED CONTENT

**S Supporting Information.** Four figures presenting competition kinetics, competition of the 3' extended constructs, and the gel-shift-monitored association and dissociation of DsrA and OxyS sRNAs to Hfq. This material is available free of charge via the Internet at <http://pubs.acs.org>.

## ■ AUTHOR INFORMATION

### Corresponding Author

\*Phone: +48-61-8528503. Fax: +48-61-8520532. E-mail: miko-laj@ibch.poznan.pl.

## Funding Sources

This work was supported by the Ministry of Science and Higher Education Grant No. N301 110 32/3871 and the “Homings” grant of the Foundation for Polish Science.

## ■ ACKNOWLEDGMENT

I thank Olke Uhlenbeck, Andrew Feig, Sarah Woodson, Sarah Ledoux, and Richard Fahlman for helpful discussions and O.U., S.L., and R.F. for critical reading of the manuscript.

## ■ ABBREVIATIONS

sRNA, small bacterial regulatory RNA; nt, nucleotides; PAGE, polyacrylamide gel electrophoresis.

## ■ REFERENCES

- (1) Waters, L. S., and Storz, G. (2009) Regulatory RNAs in bacteria. *Cell* 136, 615–628.
- (2) Romby, P., Vandenesch, F., and Wagner, E. G. (2006) The role of RNAs in the regulation of virulence-gene expression. *Curr. Opin. Microbiol.* 9, 229–236.
- (3) Altuvia, S., Weinstein-Fischer, D., Zhang, A., Postow, L., and Storz, G. (1997) A small, stable RNA induced by oxidative stress: role as a pleiotropic regulator and antimitator. *Cell* 90, 43–53.
- (4) Sledjeski, D. D., Gupta, A., and Gottesman, S. (1996) The small RNA, DsrA, is essential for the low temperature expression of RpoS during exponential growth in *Escherichia coli*. *EMBO J.* 15, 3993–4000.
- (5) Rice, P. W., and Dahlberg, J. E. (1982) A gene between *polA* and *glnA* retards growth of *Escherichia coli* when present in multiple copies: physiological effects of the gene for spot 42 RNA. *J. Bacteriol.* 152, 1196–1210.
- (6) Moller, T., Franch, T., Udesen, C., Gerdes, K., and Valentin-Hansen, P. (2002) Spot 42 RNA mediates discoordinate expression of the *E. coli* galactose operon. *Genes Dev.* 16, 1696–1706.
- (7) Udekwu, K. I., Darfeuille, F., Vogel, J., Reimegard, J., Holmqvist, E., and Wagner, E. G. (2005) Hfq-dependent regulation of OmpA synthesis is mediated by an antisense RNA. *Genes Dev.* 19, 2355–2366.
- (8) Soper, T., Mandin, P., Majdalani, N., Gottesman, S., and Woodson, S. A. (2010) Positive regulation by small RNAs and the role of Hfq. *Proc. Natl. Acad. Sci. U.S.A.*
- (9) Urban, J. H., and Vogel, J. (2007) Translational control and target recognition by *Escherichia coli* small RNAs *in vivo*. *Nucleic Acids Res.* 35, 1018–1037.
- (10) Schumacher, M. A., Pearson, R. F., Moller, T., Valentin-Hansen, P., and Brennan, R. G. (2002) Structures of the pleiotropic translational regulator Hfq and an Hfq-RNA complex: a bacterial Sm-like protein. *EMBO J.* 21, 3546–3556.
- (11) Zhang, A., Wassarman, K. M., Ortega, J., Steven, A. C., and Storz, G. (2002) The Sm-like Hfq protein increases OxyS RNA interaction with target mRNAs. *Mol. Cell* 9, 11–22.
- (12) Geissmann, T. A., and Touati, D. (2004) Hfq, a new chaperoning role: binding to messenger RNA determines access for small RNA regulator. *EMBO J.* 23, 396–405.
- (13) Moller, T., Franch, T., Hojrup, P., Keene, D. R., Bachinger, H. P., Brennan, R. G., and Valentin-Hansen, P. (2002) Hfq: a bacterial Sm-like protein that mediates RNA-RNA interaction. *Mol. Cell* 9, 23–30.
- (14) Mikulecky, P. J., Kaw, M. K., Brescia, C. C., Takach, J. C., Sledjeski, D. D., and Feig, A. L. (2004) *Escherichia coli* Hfq has distinct interaction surfaces for DsrA, rpoS and poly(A) RNAs. *Nat. Struct. Mol. Biol.* 11, 1206–1214.
- (15) Hopkins, J. F., Panja, S., and Woodson, S. A. (2011) Rapid binding and release of Hfq from ternary complexes during RNA annealing. *Nucleic Acids Res.*

- (16) Lease, R. A., and Woodson, S. A. (2004) Cycling of the Sm-like protein Hfq on the DsrA small regulatory RNA. *J. Mol. Biol.* 344, 1211–1223.
- (17) Fender, A., Elf, J., Hampel, K., Zimmermann, B., and Wagner, E. G. (2010) RNAs actively cycle on the Sm-like protein Hfq. *Genes Dev.* 24, 2621–2626.
- (18) Moll, I., Afonyushkin, T., Vytvytska, O., Kabardin, V. R., and Blasi, U. (2003) Coincident Hfq binding and RNase E cleavage sites on mRNA and small regulatory RNAs. *RNA* 9, 1308–1314.
- (19) Link, T. M., Valentin-Hansen, P., and Brennan, R. G. (2009) Structure of Escherichia coli Hfq bound to polyribadenylate RNA. *Proc. Natl. Acad. Sci. U.S.A.* 106, 19292–19297.
- (20) Sun, X., and Wartell, R. M. (2006) Escherichia coli Hfq binds A18 and DsrA domain II with similar 2:1 Hfq6/RNA stoichiometry using different surface sites. *Biochemistry* 45, 4875–4887.
- (21) de Haseth, P. L., and Uhlenbeck, O. C. (1980) Interaction of Escherichia coli host factor protein with oligoriboadenylates. *Biochemistry* 19, 6138–6146.
- (22) Soper, T. J., and Woodson, S. A. (2008) The rpoS mRNA leader recruits Hfq to facilitate annealing with DsrA sRNA. *RNA* 14, 1907–1917.
- (23) Salim, N. N., and Feig, A. L. (2010) An upstream Hfq binding site in the fhfA mRNA leader region facilitates the OxyS-fhfA interaction. *PLoS One* 5, pii: e13028.
- (24) Lorenz, C., Gesel, T., Zimmermann, B., Schoeberl, U., Bilusic, I., Rajkowitsch, L., Waldsich, C., von Haeseler, A., and Schroeder, R. (2010) Genomic SELEX for Hfq-binding RNAs identifies genomic aptamers predominantly in antisense transcripts. *Nucleic Acids Res.*
- (25) Arluison, V., Hohng, S., Roy, R., Pellegrini, O., Regnier, P., and Ha, T. (2007) Spectroscopic observation of RNA chaperone activities of Hfq in post-transcriptional regulation by a small non-coding RNA. *Nucleic Acids Res.* 35, 999–1006.
- (26) Brescia, C. C., Mikulecky, P. J., Feig, A. L., and Sledjeski, D. D. (2003) Identification of the Hfq-binding site on DsrA RNA: Hfq binds without altering DsrA secondary structure. *RNA* 9, 33–43.
- (27) Darfeuille, F., Unoson, C., Vogel, J., and Wagner, E. G. (2007) An antisense RNA inhibits translation by competing with standby ribosomes. *Mol. Cell* 26, 381–392.
- (28) Majdalani, N., Hernandez, D., and Gottesman, S. (2002) Regulation and mode of action of the second small RNA activator of RpoS translation, RprA. *Mol. Microbiol.* 46, 813–826.
- (29) Zhang, A., Altuvia, S., Tiwari, A., Argaman, L., Hengge-Aronis, R., and Storz, G. (1998) The OxyS regulatory RNA represses rpoS translation and binds the Hfq (HF-I) protein. *EMBO J.* 17, 6061–6068.
- (30) Antal, M., Bordeau, V., Douchin, V., and Felden, B. (2005) A small bacterial RNA regulates a putative ABC transporter. *J. Biol. Chem.* 280, 7901–7908.
- (31) Milligan, J. F., Groebe, D. R., Witherell, G. W., and Uhlenbeck, O. C. (1987) Oligoribonucleotide synthesis using T7 RNA polymerase and synthetic DNA templates. *Nucleic Acids Res.* 15, 8783–8798.
- (32) Fahlman, R. P., and Uhlenbeck, O. C. (2004) Contribution of the esterified amino acid to the binding of aminoacylated tRNAs to the ribosomal P- and A-sites. *Biochemistry* 43, 7575–7583.
- (33) Wong, I., and Lohman, T. M. (1993) A double-filter method for nitrocellulose-filter binding: application to protein-nucleic acid interactions. *Proc. Natl. Acad. Sci. U.S.A.* 90, 5428–5432.
- (34) Updegrove, T., Wilf, N., Sun, X., and Wartell, R. M. (2008) Effect of Hfq on RprA-rpoS mRNA pairing: Hfq-RNA binding and the influence of the 5' rpoS mRNA leader region. *Biochemistry* 47, 11184–11195.
- (35) Zhang, A., Wassarman, K. M., Rosenow, C., Tjaden, B. C., Storz, G., and Gottesman, S. (2003) Global analysis of small RNA and mRNA targets of Hfq. *Mol. Microbiol.* 50, 1111–1124.
- (36) de Haseth, P. L., and Uhlenbeck, O. C. (1980) Interaction of Escherichia coli host factor protein with Q beta ribonucleic acid. *Biochemistry* 19, 6146–6151.
- (37) Carmichael, G. G., Weber, K., Niveleau, A., and Wahba, A. J. (1975) The host factor required for RNA phage Qbeta RNA replication in vitro. Intracellular location, quantitation, and purification by polyadenylate-cellulose chromatography. *J. Biol. Chem.* 250, 3607–3612.
- (38) Hopkins, J. F., Panja, S., McNeil, S. A., and Woodson, S. A. (2009) Effect of salt and RNA structure on annealing and strand displacement by Hfq. *Nucleic Acids Res.*
- (39) Zuker, M. (2003) Mfold web server for nucleic acid folding and hybridization prediction. *Nucleic Acids Res.* 31, 3406–3415.
- (40) Bassi, G. S., and Weeks, K. M. (2003) Kinetic and thermodynamic framework for assembly of the six-component bI3 group I intron ribonucleoprotein catalyst. *Biochemistry* 42, 9980–9988.
- (41) Ho, Y., and Waring, R. B. (1999) The maturase encoded by a group I intron from Aspergillus nidulans stabilizes RNA tertiary structure and promotes rapid splicing. *J. Mol. Biol.* 292, 987–1001.
- (42) Rose, M. A., and Weeks, K. M. (2001) Visualizing induced fit in early assembly of the human signal recognition particle. *Nat. Struct. Biol.* 8, 515–520.
- (43) Olejniczak, M., Dale, T., Fahlman, R. P., and Uhlenbeck, O. C. (2005) Idiosyncratic tuning of tRNAs to achieve uniform ribosome binding. *Nat. Struct. Mol. Biol.* 12, 788–793.
- (44) Vecerek, B., Beich-Frandsen, M., Resch, A., and Blasi, U. (2010) Translational activation of rpoS mRNA by the non-coding RNA DsrA and Hfq does not require ribosome binding. *Nucleic Acids Res.* 38, 1284–1293.
- (45) Lee, T., and Feig, A. L. (2008) The RNA binding protein Hfq interacts specifically with tRNAs. *RNA* 14, 514–523.
- (46) Rolle, K., Zywicki, M., Wyszko, E., Barciszewska, M. Z., and Barciszewski, J. (2006) Evaluation of the dynamic structure of DsrA RNA from E. coli and its functional consequences. *J. Biochem.* 139, 431–438.
- (47) Hwang, W., Arluison, V., and Hohng, S. (2011) Dynamic competition of DsrA and rpoS fragments for the proximal binding site of Hfq as a means for efficient annealing. *Nucleic Acids Res.*
- (48) Afonyushkin, T., Vecerek, B., Moll, I., Blasi, U., and Kabardin, V. R. (2005) Both RNase E and RNase III control the stability of sodB mRNA upon translational inhibition by the small regulatory RNA RyhB. *Nucleic Acids Res.* 33, 1678–1689.
- (49) Galluppi, G. R., and Richardson, J. P. (1980) ATP-induced changes in the binding of RNA synthesis termination protein Rho to RNA. *J. Mol. Biol.* 138, 513–539.
- (50) Steinmetz, E. J., and Platt, T. (1994) Evidence supporting a tethered tracking model for helicase activity of Escherichia coli Rho factor. *Proc. Natl. Acad. Sci. U.S.A.* 91, 1401–1405.
- (51) Sledjeski, D. D., Whitman, C., and Zhang, A. (2001) Hfq is necessary for regulation by the untranslated RNA DsrA. *J. Bacteriol.* 183, 1997–2005.
- (52) Record, M. T., Jr., Lohman, M. L., and De Haseth, P. (1976) Ion effects on ligand-nucleic acid interactions. *J. Mol. Biol.* 107, 145–158.
- (53) Hussein, R., and Lim, H. N. (2011) Disruption of small RNA signaling caused by competition for Hfq. *Proc. Natl. Acad. Sci. U.S.A.* 108, 1110–1115.
- (54) Papenfort, K., Said, N., Welsink, T., Lucchini, S., Hinton, J. C., and Vogel, J. (2009) Specific and pleiotropic patterns of mRNA regulation by ArcZ, a conserved, Hfq-dependent small RNA. *Mol. Microbiol.* 74, 139–158.
- (55) Kajitani, M., Kato, A., Wada, A., Inokuchi, Y., and Ishihama, A. (1994) Regulation of the Escherichia coli hfq gene encoding the host factor for phage Q beta. *J. Bacteriol.* 176, 531–534.